



Liposome accumulation in irradiated tumors display important tumor and dose dependent differences

Hansen, Anders Elias; Fliedner, Frederikke Petrine; Henriksen, Jonas Rosager; Jørgensen, Jesper Tranekjær; Clemmensen, Andreas Ettrup; Børresen, Betina; Elema, Dennis Ringkjøbing; Kjær, Andreas ; Andresen, Thomas Lars

Published in:
Nanomedicine: Nanotechnology, Biology and Medicine

Link to article, DOI:
[10.1016/j.nano.2017.08.013](https://doi.org/10.1016/j.nano.2017.08.013)

Publication date:
2018

Document Version
Peer reviewed version

[Link back to DTU Orbit](#)

Citation (APA):
Hansen, A. E., Fliedner, F. P., Henriksen, J. R., Jørgensen, J. T., Clemmensen, A. E., Børresen, B., ... Andresen, T. L. (2018). Liposome accumulation in irradiated tumors display important tumor and dose dependent differences. *Nanomedicine: Nanotechnology, Biology and Medicine*, 14, 27–34. DOI: [10.1016/j.nano.2017.08.013](https://doi.org/10.1016/j.nano.2017.08.013)

General rights

Copyright and moral rights for the publications made accessible in the public portal are retained by the authors and/or other copyright owners and it is a condition of accessing publications that users recognise and abide by the legal requirements associated with these rights.

- Users may download and print one copy of any publication from the public portal for the purpose of private study or research.
- You may not further distribute the material or use it for any profit-making activity or commercial gain
- You may freely distribute the URL identifying the publication in the public portal

If you believe that this document breaches copyright please contact us providing details, and we will remove access to the work immediately and investigate your claim.



ELSEVIER

Nanomedicine: Nanotechnology, Biology, and Medicine
xx (2017) xxx–xxx

nanomedicine
Nanotechnology, Biology, and Medicine

nanomedjournal.com

Q1 Liposome accumulation in irradiated tumors display important tumor and 2 dose dependent differences

Q2 Anders Elias Hansen, DVM, PhD^{a,b,c,1}, Frederikke Petrine Fliedner, MSc^{b,c,1},
4 Jonas Rosager Henriksen, MSc, PhD^{b,d}, Jesper Tranekjær Jørgensen, MSc, PhD^c,
5 Andreas Ettrup Clemmensen, MSc^c, Betina Børresen, DVM^{a,e},
6 Dennis Ringkjøbing Elema, MSc, PhD^f, Andreas Kjær, MD, DMSc, PhD^c,
7 Thomas Lars Andresen, MSc, PhD, Prof^{a,b,*}

^aDepartment of Micro- and Nanotechnology, DTU Nanotech, Technical University of Denmark, Kongens Lyngby, Denmark

^bCenter for Nanomedicine and Theranostics, Technical University of Denmark, Kongens Lyngby, Denmark

^cDepartment of Clinical Physiology, Nuclear Medicine & PET and Cluster for Molecular Imaging, Department of Biomedical Sciences, Rigshospitalet and
11 University of Copenhagen, Copenhagen, Denmark

^dDepartment of Chemistry, DTU Chemistry, Technical University of Denmark, Kongens Lyngby, Denmark

^eDepartment of Small Animal Clinical Sciences, Copenhagen University, Frederiksberg, Denmark

^fHevesy Laboratory, DTU Nutech, Technical University of Denmark, Roskilde, Denmark

Received 29 March 2016; accepted 21 August 2017

16 Abstract

17 Radiation therapy may affect several important parameters in the tumor microenvironment and thereby influence the accumulation of
18 liposomes by the enhanced permeability and retention (EPR)-effect. Here we investigate the effect of single dose radiation therapy on
19 liposome tumor accumulation by PET/CT imaging using radiolabeled liposomes. Head and neck cancer xenografts (FaDu) and syngenic
20 colorectal (CT26) cancer models were investigated. Radiotherapy displayed opposite effects in the two models. FaDu tumors displayed
21 increased mean accumulation of liposomes for radiation doses up to 10 Gy, whereas CT26 tumors displayed a tendency for decreased
22 accumulation. Tumor hypoxia was found negatively correlated to microregional distribution of liposomes. However, liposome distribution in
23 relation to hypoxia was improved at lower radiation doses. The study reveals that the heterogeneity in liposome tumor accumulation between
24 tumors and different radiation protocols are important factors that need to be taken into consideration to achieve optimal effect of liposome
25 based radio-sensitizer therapy.

26 © 2017 Elsevier Inc. All rights reserved.

27 *Key words:* Liposome; PET; Radiotherapy; Radio-sensitizer; Hypoxia

28 External beam radiation therapy (RT) is a central part of the
29 treatment regimen for more than half of all cancer patients.
30 Liposomal drug delivery systems that carry radio-sensitizers to

tumors can potentially improve therapeutic efficacy of RT 31
without increasing loco-regional side effects in the irradiated 32
region.^{1,2} Combining targeted RT and targeted drug delivery can 33
therefore increase regional tumor control.³ Moreover, liposomes 34
are flexible in regards to the selection of drugs that can be 35
encapsulated, transported and released within tumors. Lipo- 36
somes can therefore serve as optimal delivery systems for 37
targeting radiosensitizers to malignant tissue.^{1,2} However, 38
liposome accumulation in solid tumors has been demonstrated 39
to depend on multiple factors, including interstitial pressure, 40
tumor vasculature and perfusion.^{4–6} Liposome extravasation by 41
the enhanced permeability and retention (EPR) effect is primarily 42
driven by transvascular convection and their accumulation is 43
44
45
46
47
48
49
50
51
52
53
54

Conflict of interest: There are no conflicts of interest.

Funding: The support from the European Research Council, the Novo Nordisk Foundation, the Lundbeck Foundation, the Innovation Fund Denmark, the Research Council of Independent Research, the Svend Andersen Foundation and the Arvid Nilsson Foundation is gratefully acknowledged.

*Corresponding author at: Department of Micro- and Nanotechnology, Building 3450, room 050, DK-2800 Kongens Lyngby.

E-mail address: thomas.andresen@nanotech.dtu.dk (T.L. Andresen).

¹ These Authors contributed equally to this work.

<http://dx.doi.org/10.1016/j.nano.2017.08.013>

1549-9634/© 2017 Elsevier Inc. All rights reserved.

inversely correlated to interstitial fluid pressure (IFP) and directly correlated to regional blood perfusion and leakiness.^{4,6–8} RT influences these parameters; however, results on the effect on tumor accumulation levels of nano-sized particles are not clear.⁶

Molecular oxygen is the most important radio-sensitizer and hypoxic tumor cells are highly radio-resistant and display increased malignancy. Tumor hypoxia is generally divided in acute perfusion limited, chronic diffusion limited and anemic hypoxic.⁹ The nature of tumor hypoxia is closely related to vascular parameters and liposomes may therefore distribute poorly to hypoxic regions. In both experimental and clinical tumors the IFP is increased and associated with an increased malignant phenotype.^{10,11} RT has been associated with increased vascular leakiness, and high total radiation doses can potentially increase the extravasation of macromolecules.⁶ Pretreating tumors with cytotoxic agents has been identified to increase tumor blood flow and decrease IFP, potentially being the results of a reduction in tumor cell density to alleviate tumor blood vessels compressions and increase the vascular surface area which subsequently increases liposome accumulation.^{12,13} Following these observations the effects of RT could also mediate a beneficial effect for macromolecular extravasation by reducing cell density.^{11,14} Importantly, single radiation doses >10 Gy, are known to cause significant damage to neoangiogenic tumor vasculature and increase hypoxia and mediate significant secondary cancer cell death following vascular damage.¹⁵ On the contrary, single doses <10 Gy cause mild vascular damage and may potentially increase vascular perfusion and thereby decrease hypoxia after irradiation.^{15–17} Few studies of the effect of RT on liposome uptake have been conducted. Single-fraction irradiation had no effect on liposome uptake in human KB cancer xenografts when evaluated by gamma counting radiolabeled liposomes.¹⁸ Considering this and that important tumor dependent differences and responses may exist, we investigated the effect of single fraction radiation therapy on liposome accumulation. This was evaluated by non-invasive PET imaging in regard to i) the potential for improving liposomal drug delivery by RT 24 h prior to liposome administration, ii) the influence of RT on vascular tumor parameters, cellular density and necrosis and iii) locoregional liposome accumulation in hypoxic tumor regions, in a human head and neck cancer xenograft model and in a syngenic murine colon cancer model.

Methods

Tumor model

FaDu (human head and neck cancer) xenografts were established by subcutaneous injection of $\sim 5 \times 10^6$ cells suspended in 100 μ l of culture medium and Matrigel over the thigh/flank of 7 weeks old female NMRI nude mice. Tumors were allowed to grow for 12–14 days. CT26 (murine colon cancer) syngenic tumors were established by subcutaneous injection of $\sim 3 \times 10^5$ cells suspended in 100 μ l of culture medium over the thigh/flank of 6 weeks old female Balb/c mice.

Tumors were allowed to grow for 18 days. The National Animal Experiments Inspectorate approved all study procedures.

Radiolabeled liposomes

Pegylated liposomes consisting of HSPC:CHOL:DSPE-PEG2k (56.5:38.2:5.3) were remote loaded with the PET isotope $^{64}\text{Cu}^{2+}$. Briefly, 100 nm 50 mM pegylated liposomes entrapping 10 mM DOTA were prepared as previously described.¹⁹ Radiolabelling was achieved by adding a volume of liposomes to dried $^{64}\text{CuCl}_2$ followed by incubation at 55 °C for 75 min. The loading efficiency was afterward evaluated by Thin Layer Chromatography (Radio-TLC) and Size Exclusion Chromatography (Radio-SEC),¹⁹ which showed a loading efficiency of >98% for both techniques. The liposomes were prepared at either 3.3 mM or 6.6 mM lipid concentration and an activity concentration of 62.5 MBq/ml or 125 MBq/ml (activity at the time of injection) for the FaDu and CT26 tumors respectively. Each animal was dosed with a volume corresponding to 22 μ mol/kg and an activity of ~ 12.5 MBq/animal.

Radiation therapy

Mice carrying FaDu xenografts were randomized into four treatment groups; non-irradiated controls (n = 11), 5 Gy (n = 11), 10 Gy (n = 10) and 20 Gy (n = 11). Mice carrying CT26 tumors were randomized into four treatment groups; non-irradiated controls (n = 8), 2 Gy (n = 8), 5 Gy (n = 8) and 10 Gy (n = 8). Radiation therapy was delivered as a single fraction at a dose-rate of 1 Gy/min (320 kV, 12.5 mA) using a small animal irradiator (X-rad320, pXi, CT, USA). Mice were irradiated in a dedicated fixation device securing that only the tumor bearing leg was exposed to irradiation and the remaining body shielded.

MicroPET/CT imaging

PET/CT imaging was performed on an Inveon® small animal PET/CT system (Siemens Medical Systems, PA, USA) approximately 24 h after completion of RT. Mice were anesthetized by inhalation anesthesia ($\sim 3\%$ sevoflurane) and ^{64}Cu -liposomes injected into a tail vein. ^{64}Cu -liposomes were allowed to distribute for 1 h before commencing a 5-min PET scan (1-h scan) followed by a corresponding CT scan. A similar PET/CT scan (15 min acquisition) was performed after a distribution period of 24 h (24-h scan). Emission data were corrected for dead time and decay and attenuation correction was performed based on the corresponding CT scan. PET scans were reconstructed using a maximum a posteriori (MAP) reconstruction algorithm (0.815 \times 0.815 \times 0.796 mm). Image analysis was performed using Inveon® software (Siemens Medical Systems, PA, USA). 3D regions of interest (ROIs) were manually constructed and decay corrected data (%injected dose per gram tissue (%ID/g)) reported.

Immunohistochemistry CD31, cell density and necrosis

Immunohistochemistry (IHC) was performed on formalin-fixed, paraffin-embedded 4 μ m tumor sections that were stained with H&E for histological evaluation and with CD31 antibodies for tumor blood vessels. CD31 staining was performed by

162 heating sections at 60 °C (1 h) followed by deparaffination in
 163 xylene and rehydration. Antigen retrieval was performed by
 164 microwave-based antigen retrieval. Endogenous peroxidase
 165 was blocked using peroxidase blocking reagent (Dako, Glostrup,
 166 Denmark) for 8 min and sections blocked in 2% BSA for (10
 167 min). Sections were incubated with primary CD31 antibody
 168 (Abcam, diluted 1:100) in 2% BSA (1.5 h/room temperature)
 169 followed by incubation with secondary biotinylated EnVision
 170 FLEX™ (40 min) (Dako, Glostrup, Denmark). Tissue sections
 171 were stained with DAB (10 min) and counterstained with
 172 hematoxylin. Between all steps sections were rinsed in PBS.

173 Slides were mounted for electronic slide scanning (Axio scan,
 174 Carl Zeiss, Germany) (pixel size 0.022 × 0.022 μm). Tumor
 175 necrosis was evaluated using the Advanced Weka segmentation
 176 plug-in for Fiji (ImageJ). The degree of necrosis in sections was
 177 determined by drawing ROIs in necrotic, background/artifacts
 178 and viable tumor region and transferring these to the trainable
 179 classifier to determine necrotic and viable areas.

180 Ten regions were selected on CD31 stained sections and sent
 181 for analysis of microvessel density by automated segmentation
 182 algorithm for analysis of microvessels in immunostained
 183 histological tumor sections (CAncer IMage ANalysis: <http://www.caiman.org.uk>).^{20,21} The regions were additionally trans-
 184 ferred to Fiji (ImageJ) for determination of nuclear density. In
 185 short, color deconvolution was performed to yield a separate
 186 hematoxylin image and the nuclei density determined by
 187 excluding fragments and artifacts by automated exclusion of
 188 structures below a cut-off size of (50 pixels²).
 189

190 ⁶⁴Cu-liposome autoradiography and hypoxia immunohisto- 191 chemistry

192 For analysis of intratumoral distribution of liposomes and
 193 hypoxia FaDu tumors (controls) were intravenously injected
 194 with the radiolabeled liposomes and these were allowed to
 195 distribute for 24 h before sacrificing and bleeding mice. To
 196 further study the influence of radiation therapy on intratumoral
 197 hypoxia and liposome distribution, tumors from and two CT26
 198 tumors from each group were subjected to autoradiography and
 199 hypoxia immunohistochemistry (26 h distribution period for
 200 liposomes). For hypoxia immunohistochemistry the exogenous
 201 hypoxia marker Pimonidazole (60 mg (kg animal)⁻¹ in PBS),
 202 was administered by intraperitoneal injection two hours before
 203 sacrifice. After sacrificing and bleeding animals, tumors were
 204 snap frozen and cryosectioned (8 μm) in cutting media. Sections
 205 separated by at least 400 μm were thaw mounted on Superfrost
 206 Plus microscopy slides. Seventeen sections from eight different
 207 FaDu tumors and five sections from included CT26 tumors were
 208 evaluated. Intratumoral distribution of ⁶⁴Cu-liposomes was
 209 determined by exposing tumor sections to phosphor imaging
 210 screens for approximately 18 h (−20 °C). Phosphor screen was
 211 read using a phosphor imaging system (Cyclone Plus, Perkin
 212 Elmer, MA, USA) and semi-quantitative luminescence images
 213 (pixel size 0.04 × 0.04 mm) were obtained.

214 Tumor sections were fixed in acetone (4 °C/10 min). Tissue
 215 peroxidase was quenched using peroxidase blocker (Dako,
 216 Glostrup, Denmark) and non-specific binding blocked using 2%
 217 BSA. Pimonidazole immunohistochemistry was performed

using mouse monoclonal anti-pimonidazole antibody (Hypoxyp- 218
 robe, MA, USA) diluted in 2% BSA (1:600) (1 h) followed by 219
 Secondary biotinylated anti-mouse antibody (40 min) (Envision 220
 Flex, Dako, Glostrup, Denmark). Antibody binding was 221
 visualized using DAB and sections were counterstained with 222
 hematoxylin (H) and slide scanned as described above. 223

ROIs, including viable tumor regions and excluding necrotic 224
 regions and artifacts were manually drawn (Fiji, ImageJ, NIH, 225
 MD, USA). Automated DAB-H color deconvolution and manual 226
 thresholding of pimonidazole IHC staining followed by image 227
 binarization was performed in Fiji software. Autoradiography 228
 images were co-registered to the corresponding pimonidazole 229
 DAB-H images using a rigid co-registration algorithm 230
 (MATLAB 8.4, The MathWorks, Inc., MA, United States). 231
 Pimonidazole values on rescaled image (autoradiography 232
 resolution) represent mean level pimonidazole positive pixels 233
 on the constructed binarized image. ⁶⁴Cu-liposome autoradiog- 234
 raphy pixels were categorized into four activity levels (0-0.25, 235
 0.26-0.50, 0.51-0.75 and 0.76-1.0) relative to the individual slide 236
 single pixel maximum. The corresponding mean pimonidazole 237
 pixel values for the four ⁶⁴Cu-Liposome categories were 238
 determined for each slide and bar-plots constructed. 239

240 *Statistical analysis*

Prism 7 (GraphPad Software, La Jolla, CA., USA) was used 241
 for all statistical analysis. One-way or two-way ANOVA 242
 analysis and Holm–Sidak multiple comparison test were applied 243
 for comparisons of groups. All data are reported as mean ± SEM 244
 (standard error of mean) unless otherwise stated and a *P*-value 245
 <0.05 considered statistically significant. 246

247 **Results**

248 *⁶⁴Cu-liposome PET/CT after radiation therapy*

Radiation therapy was successfully delivered to all mice 249
 before administration of radiolabeled liposomes. The treatment 250
 schedule was chosen to ensure that the acute effect of irradiation 251
 was activity during the period of liposome distribution. To 252
 evaluate the effects of the different radiation doses we extracted 253
 tumor activity levels of ⁶⁴Cu-liposome PET data from the 254
 co-registered PET/CT images from the 1-h and 24-h PET/CT 255
 scans. Two PET scans were performed to extract information on 256
 accumulation, as intravascular liposome activity is expected to 257
 dominate the 1-h PET scan and liposomes that have extravasated 258
 through fenestrated tumor blood vessels the 24-h scan. PET/CT 259
 images from the 24-h scans from each treatment group are 260
 illustrated in [Figure 1, A-H](#). 261

FaDu tumors displayed no significant ⁶⁴Cu-liposome activity 262
 difference between controls and treatment groups at the 1-h PET/
 CT ([Figure 2, A and B](#)). At the 24-h PET/CT FaDu tumors 263
 receiving 5 Gy and 10 Gy had significantly higher mean 264
 liposome activity compared to the control group, while no 265
 liposome activity was observed for the mean activity of the 20 266
 Gy treatment group ([Figure 2, C](#)). For the comparison of the 24-h 267
 maximum activity, only the 5 Gy treatment group was 268
 statistically higher than the control group ([Figure 2, D](#)). The 270

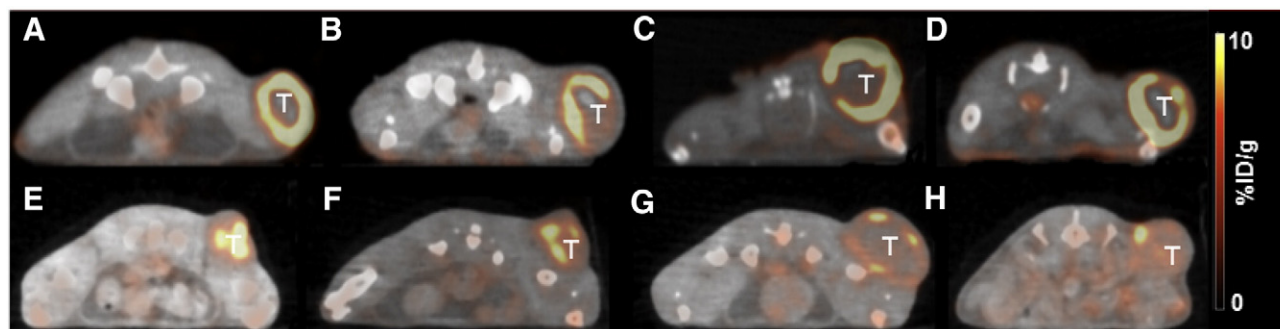


Figure 1. ^{64}Cu -liposome PET/CT of FaDu xenografts (top row) (A) non-irradiated control (n = 11), (B) 5 Gy (n = 11), (C) 10 Gy (n = 10), (D) 20Gy (n = 11) and CT26 tumors (bottom row) (E) non-irradiated control (n = 8), (F) 2 Gy (n = 8), (G) 5 Gy (n = 8), (H) 20 Gy (n = 8). (T) Tumor.

271 influence of radiation on liposome accumulation was further
 272 investigated in the syngenic CT26 tumors. Following the higher
 273 radiosensitivity in comparison to FaDu tumors, an irradiation
 274 schedule of 2 Gy, 5 Gy and 10 Gy was chosen. Interestingly, for
 275 the CT26 tumors an inverse correlation between radiation dose
 276 and liposome accumulation was observed. There was significantly
 277 higher mean activity of liposomes in the control group
 278 compared to all treatment groups at the 1-h PET scan (Figure 2,
 279 E). The control group also displayed the highest maximum
 280 activity of ^{64}Cu -liposomes at the 1-h scan although this was not
 281 significant in comparison to irradiated groups (Figure 2, F).
 282 These observations could indicate that a high level of damage
 283 was induced to intratumoral blood vessels that limit intravascular
 284 liposome blood activity. Opposite to the observations in FaDu
 285 tumors, the irradiated CT26 groups displayed lower activity
 286 levels in comparison to controls. This was however only
 287 statistically significant for the controls in comparison to the 5
 288 Gy irradiated group (Figure 2, G and H). Based on the
 289 conflicting results of the liposome uptake in the two included
 290 tumor models we evaluated the effect of radiation dose on tumor
 291 parameters that are expected to influence liposome
 292 accumulation.

293 Micro vessels, nuclear density and necrosis

294 The levels of intratumoral necrosis, nuclear density and micro
 295 vessels were investigated on stained tumor sections. For the
 296 FaDu tumor we observed a higher level of intratumoral necrosis
 297 primarily in the central parts of the tumors whereas less and more
 298 scattered distribution of necrosis was observed for the CT26
 299 tumors. FaDu non-irradiated controls displayed a mean intratu-
 300 moral necrosis level of 21.6% (\pm 4.5) while CT26 tumors only
 301 displayed 11.0% (\pm 1.3). For both tumor types the level of
 302 intratumoral necrosis increased with higher doses of radiation,
 303 except for the comparison of the 5 Gy FaDu group and controls.
 304 However, only the 20 Gy FaDu group and the 5 Gy and 10 Gy
 305 CT26 groups and corresponding controls were significantly
 306 different (Figure 3, A and D). As liposome accumulation is not
 307 expected to occur in devascularized non-vital necrotic regions
 308 this could explain the observed lower activity in comparison to
 309 controls for the 20 Gy FaDu group and the irradiated groups of
 310 CT26 tumors.

Nuclear density was found to decrease with increasing 311
 radiation dose. The cell density in the treatment groups all, 312
 except for the 5 Gy FaDu group, displayed significantly lower 313
 cellular density compared to control groups for both tumor types 314
 (Figure 3, B and E). The lower cell density is expected to 315
 decrease interstitial pressure in tumors and therefore facilitate an 316
 easier extravasation of liposomes. However, this was correlated 317
 to an increased the overall ^{64}Cu -liposome accumulation. 318
 Additionally, cell density could potentially be counteracted by 319
 pressure changes stimulated by radiation-induced inflammation, 320
 apoptosis, necrosis and acute microvessel damage. 321

The micro vessel density (MVD) was investigated to identify 322
 if blood vessel density could explain the observed liposome 323
 activity differences. The MVD displayed no significant differ- 324
 ence between FaDu groups (Figure 3, C). Interestingly, the CT26 325
 control group displayed significantly higher MVD than all 326
 irradiated groups (Figure 3, F). The higher mean ^{64}Cu -liposome 327
 activity at the 1-h PET could potentially be explained by the 328
 higher microvessel density. However, for the 24-h scan this did 329
 not result in significantly higher activity, whereas the FaDu 330
 tumors displayed significantly higher activity levels for the 5 Gy 331
 and 10 Gy groups. 332

Microregional distribution of ^{64}Cu -liposomes and pimonidazole 333

To investigate the potential of liposomal drug delivery system 334
 to improve therapeutic control of radio-resistant hypoxic tumor 335
 regions we compared the accumulation of radiolabeled lipo- 336
 somes to pimonidazole hypoxia immunohistochemistry. 337
 ^{64}Cu -liposome autoradiographies were compared to of pimoni- 338
 dazole immunohistochemistry for non-irradiated FaDu tumor 339
 sections. The co-registration process and resizing of images 340
 allowed us to include seventeen sections in the analysis. The 341
 microregional pixel-to-pixel comparison of pimonidazole values 342
 and corresponding categorized ^{64}Cu -liposome activity level 343
 identified that hypoxia decreases significantly with increasing 344
 (within slide) ^{64}Cu -liposome activity (Figure 4, A-D). This 345
 observation is important for liposome based radiosensitizer 346
 therapy, as they may have limited access to important hypoxic 347
 regions at least for the liposomes under investigation. Following 348
 the observed influence of radiation cellular density and vascular 349
 function the influence of dose on pimonidazole positive fraction 350
 was investigated in CT26 tumors. We observed a significantly 351

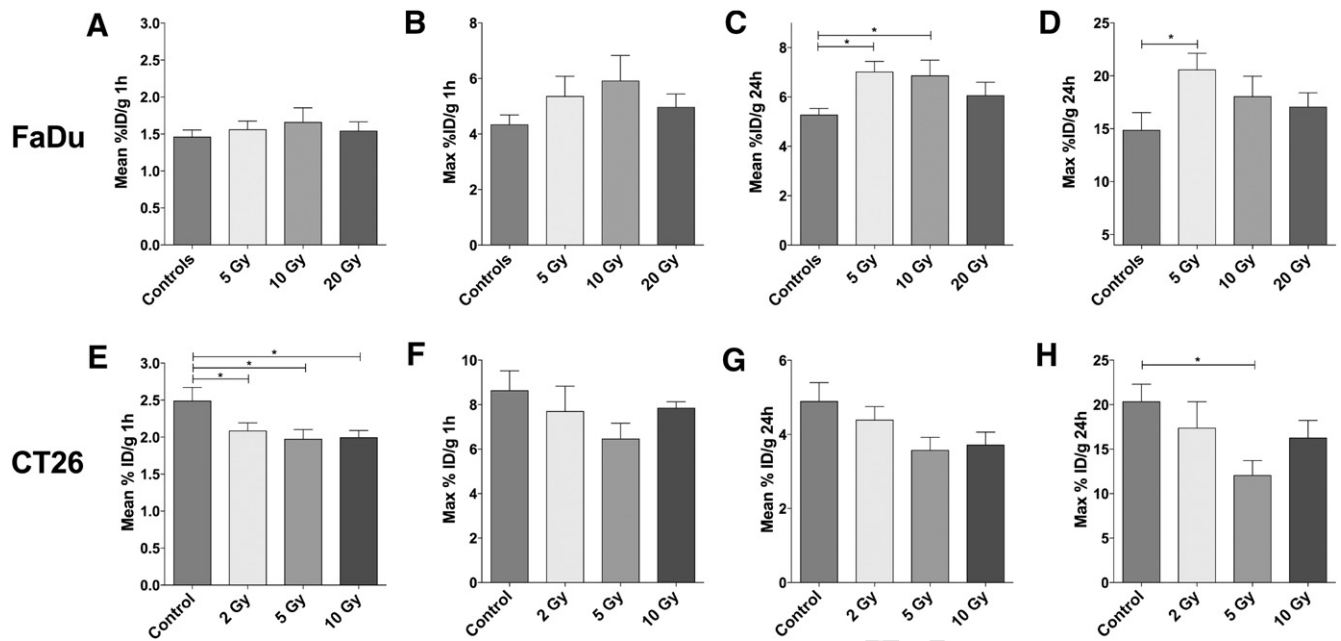


Figure 2. Tumor mean and maximum activity levels at 1-h and 24-h after injection of ^{64}Cu -liposomes evaluated by PET/CT for control and treatment groups. FaDu tumors (A-D) and CT26 tumors (E-H) (%ID/g \pm SEM) (* $P < 0.05$).

352 lower fraction of pimonidazole positive pixel in the 2 Gy
 353 irradiated group, no difference for the 5 Gy group and
 354 a significantly increased positive fraction in the 10 Gy group
 355 relative to controls (Figure 4, E). To determine if the observed
 356 changes in tumor oxygenation could influence the distribution
 357 patterns of liposomes relative to microregional hypoxia a
 358 comparison of ^{64}Cu -liposome activity level and pimonidazole
 359 was performed. The control group displayed an inverse
 360 correlation that was comparable to that of non-irradiated FaDu
 361 tumors (Figure 4, F). However, the 2 Gy and 5 Gy irradiated
 362 groups displayed an almost similar level of hypoxia in the
 363 different levels of ^{64}Cu -liposome activity, which could indicate
 364 that these dose ranges can potentially both decrease levels of
 365 hypoxia and improve liposome accumulation in regards to
 366 hypoxic areas. This must of course be weighed against the
 367 overall accumulation of ^{64}Cu -liposomes.

368 Discussion

369 The therapeutic combination of tumor targeting liposome-
 370 encapsulated radiosensitizers and radiation therapy holds great
 371 clinical potential following the dual tumor targeting properties.
 372 Notwithstanding this potential, the direct link between the
 373 parameters of central importance for liposome accumulation and
 374 the effects of radiation therapy makes the determination of
 375 optimal timing of radiation and dose and liposome administra-
 376 tion important.

377 The two cancer models yielded opposite results in respect to
 378 liposomes accumulation. Whereas radiation improved accumu-
 379 lation in FaDu xenografts after 24-h (5 Gy and 10 Gy groups),
 380 the CT26 tumors displayed an insignificant decrease in liposome
 381 accumulation after radiation. These observations are interesting

in respect to the study in human KB cancer xenografts where no
 effect, negative or positive, on liposome uptake was observed for
 radiation doses from 5 to 20 Gy evaluated invasively from 1 to
 96 h after irradiation.¹⁸ Both cancer models displayed an
 increase in intratumoral necrosis and decreased cell density
 following irradiation, both of which were most significant for the
 CT26 tumors. Interestingly, MVD was found to respond very
 differently to irradiation between the models. Irradiation
 significantly decreased MVD in CT26 while FaDu tumors did
 not display changes or patterns in relation to radiation. This was
 also illustrated by the mean ^{64}Cu -liposome activity between
 groups after a circulation period of only 1-h. In clinical head and
 neck squamous cell carcinomas a decrease in MVD was
 correlated to an improved response and overall survival.¹⁷ In
 light of this, our results indicate that the FaDu tumors represent a
 more radio-resistant tumor and that adjuvant liposomal radio-
 sensitizer therapy could be beneficial, at least from a dose
 accumulation perspective for tumors maintaining a high MVD
 during irradiation. Based on the differences in liposomes
 accumulation and the histological analysis, accumulation
 appeared directly dependent on a high MVD. This observation
 is in agreement with previous publications identifying, blood
 flow as the rate limiting step for liposome extravasation in
 tumors with a high vascular permeability.²⁵ However, irradiation
 can decrease nuclear density and damage vascular structures to
 potentially increase liposome accumulation by lowering IFP and
 facilitating transvascular extravasation. No direct measures for
 IFP in addition to nuclear density were performed but in a
 previous report on irradiation of colon carcinoma xenografts
 single fractions of 10 Gy significantly lowered IFP in tumor.²²
 From our results, the differences between MVD response and
 comparable decrease in nuclear density between FaDu and CT26
 tumors indicate that the MVD is the most important parameter to

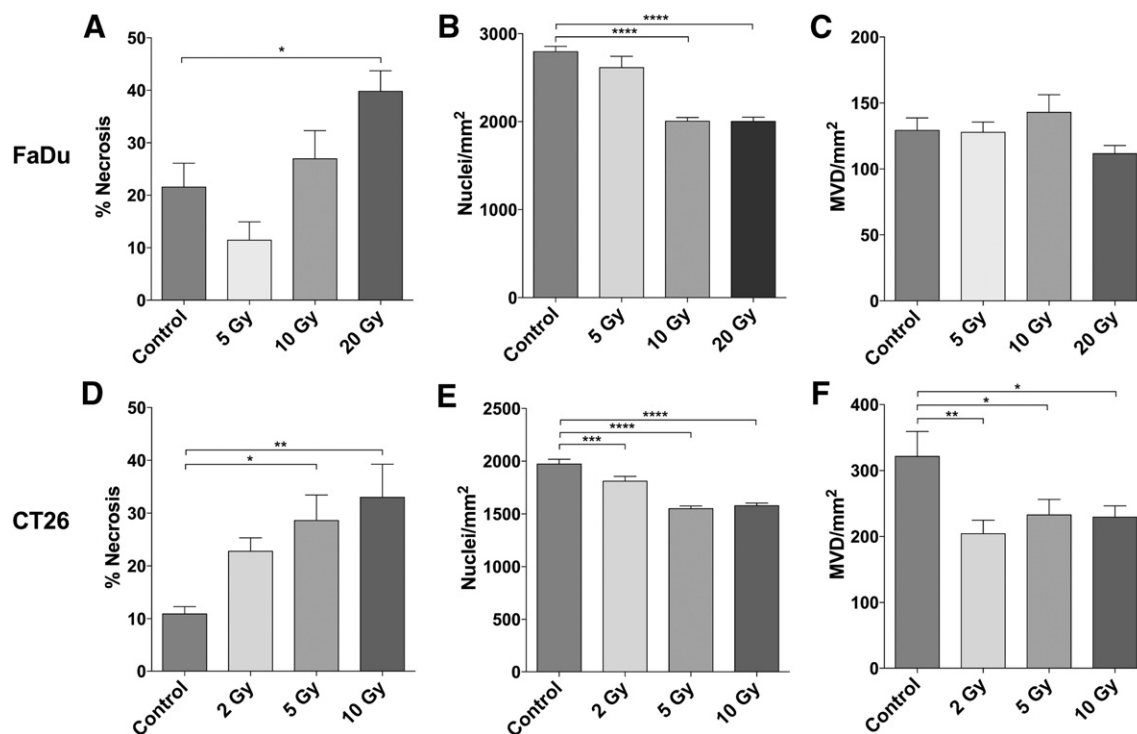


Figure 3. Immunohistochemical analysis of percentage of necrosis, nuclear counts per mm² and microvascular density (MVD/mm²) determined by automated segmentation on tumor sections from control and treatment groups (mean ± SEM). FaDu tumors (A-C). CT26 tumors (D-F) (mean ± SEM). * $P \leq 0.02$, ** $P \leq 0.005$, *** $P < 0.001$, **** $P < 0.0001$.

influence liposome accumulation. Compatible results were obtained for non-small cell lung cancer patients receiving adjuvant liposomal doxorubicin to fractionated radiotherapy where MVD was associated with increased accumulation and therapeutic efficacy.²³ However, the association of MVD to hypoxia could also influence this observation as discussed below. Interestingly, the increased liposome accumulation for irradiated FaDu tumors could also result from a decreased IFP which may improve tumor perfusion by alleviating pressure dependent collapse of intratumoral vessels.^{24,25} Importantly, the optimal timing of liposomal drug administration in relation to fractionated radiation remains to be determined and the reported negative impact of RT five days after irradiation indicates that timing is central for optimization of liposome accumulation.²² Based on our observations improving liposome accumulation is a balance between maintaining functional blood vessels and improving intratumoral blood flow as discussed in recent literature.²⁶ However, the heterogeneous response of different tumor models, in regards to these parameters, highlights the value of directly quantitative PET imaging using radiolabeled liposomes.

Single doses of (≥ 10 Gy) RT induce high levels of vascular damage that leads to secondary cell death when areas become deprived of oxygen and nutrients. On the other hand, fractionated low dose irradiation of tumors has been associated with improved perfusion and reoxygenation.¹⁵⁻¹⁷ The tumor sections evaluated from the 2 Gy and 5 Gy CT26 groups displayed less hypoxia across all levels of liposome activity, which is in line with reports on early reoxygenation after low dose irradiation. This indicates that the low dose irradiation, at least for the CT26 tumors, improves vascular perfusion and tumor oxygenation and provides the basis

for a more homogeneous distribution of liposomes. The effect of 444 radiation therapy can therefore potentially also improve liposome 445 penetration and the potential of targeting liposomes that suffers 446 from inability to reach their target if trapped in the perivascular 447 regions.⁸ Considering the importance of hypoxia and its intricate 448 link to vascularization, optimized radiation schedules can 449 potentially improve the distribution of liposomes in radioresistant 450 hypoxic region.²⁵ Liposomal doxorubicin has been reported to 451 increase radiosensitivity in hypoxic prostate cancer xenografts in 452 one study where clamping of the tumor-bearing leg was used to 453 induce hypoxia during RT. However, liposomes were adminis- 454 tered prior to clamping and the study therefore provides no 455 evidence that doxorubicin reaches regions of perfusion and 456 diffusion limited hypoxia, but highlights the potential of liposomal 457 chemoradiotherapy.²⁷ Liposomal doxorubicin and cisplatin, 458 injected 16 h before irradiation, increased the therapeutic efficacy 459 for 4.5 Gy single dose and 9 Gy/3 fractions but not a single dose of 460 9 Gy radiotherapy in KB head and neck cancer xenografts. No 461 benefit was observed from dosing liposomes as a single compared 462 to multiple injections of the same dose and the authors were not 463 able to determine if the effects observed were truly radio- 464 sensitizing or additive,²⁸ which highlights the importance of 465 timing to achieve a supra-additive effect chemoradiotherapy. 466

Conclusion

467

The present study was conducted using a radiolabeled 468 liposome imaging system that provided quantitative data on 469

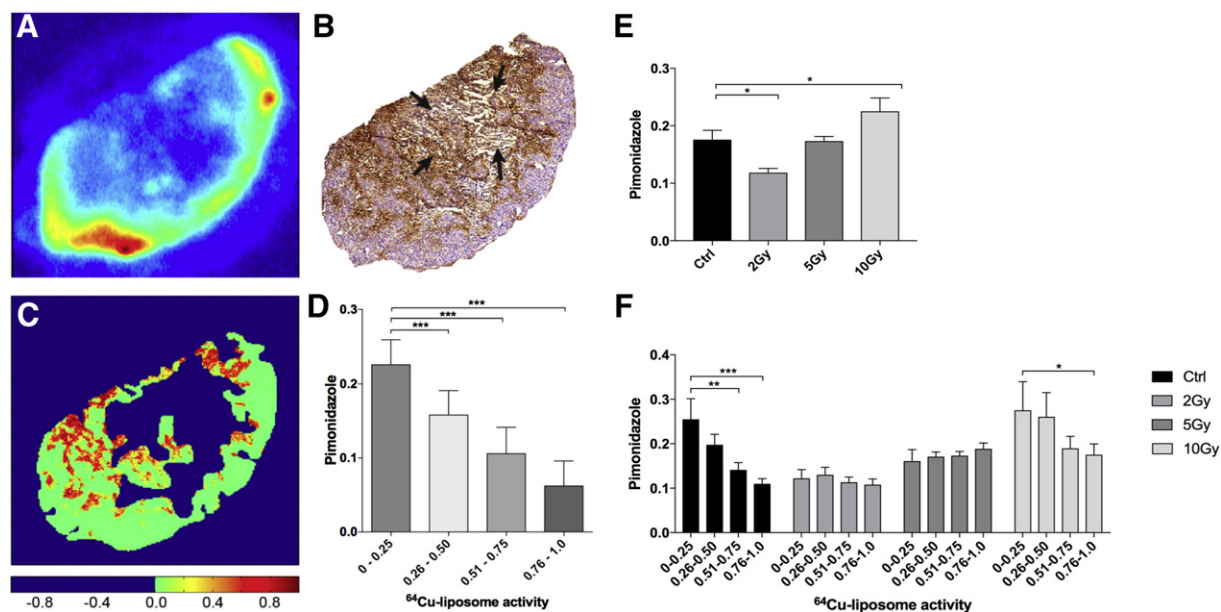


Figure 4. Microregional ^{64}Cu -liposome and pimonidazole distribution evaluated on cryosectioned tumor slides. Illustrative section from a control tumor (A) ^{64}Cu -liposome autoradiography, (B) pimonidazole peroxidase and hematoxylin (DAB-H) immunohistochemistry, black arrows indicate a central necrotic region, (C) interpolated pimonidazole image in false-color, color bar illustrates percent of pimonidazole positive pixels from a constructed binary pimonidazole image. (D) Bar plot illustrating the association between regional level of liposome and degree of pimonidazole hypoxia. Pimonidazole pixel values and the corresponding ^{64}Cu -liposome pixel activity levels categorized according to maximum pixel activity on autoradiography (mean \pm SEM). (E) Percentage of pimonidazole positive pixels (mean \pm SEM) in tumor sections from controls and irradiated CT26 tumor sections. (F) Bar plots illustrating the association between regional ^{64}Cu -liposome activity relative to section maximum and degree of pimonidazole hypoxia for the different CT26 treatment groups and controls. (* $P < 0.05$, ** $P < 0.01$, *** $P < 0.001$).

470 liposome accumulation as a function of RT. The study identifies
 471 that RT may influence the EPR effect and liposome accumula-
 472 tion in a tumor and dose dependent manner. This observation
 473 emphasizes that the ^{64}Cu -liposome PET imaging system may
 474 provide a theranostic tool to identify patients and treatment
 475 combinations and kinetics that may benefit from liposomal drug
 476 delivery in relation to radiation therapy. Future studies of
 477 liposomal drug delivery systems for radiosensitizers focusing on
 478 the correlation between liposome accumulation in tumor tissue
 479 as a function of RT and the therapeutic effect induced are highly
 480 warranted.

481 References

- 482 1. Petersen AL, Hansen AE, Gabizon A, Andresen TL. Liposome imaging
 483 agents in personalized medicine. *Adv Drug Deliv Rev* 2012;**64**:1417-
 484 1435.
- 485 2. R. I. Jolck, L. N. Feldborg, S. Andersen, S. M. Moghimi and T. L.
 486 Andresen, Engineering liposomes and nanoparticles for biological
 487 targeting. *Adv Biochem Eng Biotechnol*.125:251–80.
- 488 3. Koukourakis MI, Koukouraki S, Giatromanolaki A, Kakolyris S,
 489 Georgoulas V, Velidaki A, et al. High intratumoral accumulation of
 490 stealth liposomal doxorubicin in sarcomas—rationale for combination
 491 with radiotherapy. *Acta Oncol* 2000;**39**:207-211.
- 492 4. Li Y, Wang J, Wientjes MG, Au JL. Delivery of nanomedicines to
 493 extracellular and intracellular compartments of a solid tumor. *Adv Drug*
 494 *Deliv Rev* 2012;**64**:29-39.
- 495 5. Jain RK, Stylianopoulos T. Delivering nanomedicine to solid tumors.
 496 *Nat Rev Clin Oncol* 2010;**7**:653-664.

6. Multhoff G, Vaupel P. Radiation-induced changes in microcirculation Q5
 and interstitial fluid pressure affecting the delivery of macromolecules 498
 and nanotherapeutics to tumors. *Front Oncol* 2012;**2**:165. 499
7. Jain RK. Transport of molecules in the tumor interstitium: a review. 500
Cancer Res 1987;**47**:3039-3051. 501
8. Jain RK, Baxter LT. Mechanisms of heterogeneous distribution of 502
 monoclonal antibodies and other macromolecules in tumors: signifi- 503
 cance of elevated interstitial pressure. *Cancer Res* 1988;**48**:7022-7032. 504
9. Vaupel P. Hypoxia and aggressive tumor phenotype: implications for 505
 therapy and prognosis. *Oncologist* 2008;**13**(Suppl 3):21-26. 506
10. Yu T, Liu K, Wu Y, Fan J, Chen J, Li C, et al. High interstitial fluid 507
 pressure promotes tumor cell proliferation and invasion in oral squamous 508
 cell carcinoma. *Int J Mol Med* 2013;**32**:1093-1100. 509
11. Rofstad EK, Ruud EB, Mathiesen B, Galappathi K. Associations 510
 between radiocurability and interstitial fluid pressure in human tumor 511
 xenografts without hypoxic tissue. *Clin Cancer Res* 2010;**16**:936-945. 512
12. Griffon-Etienne G, Boucher Y, Brekken C, Suit HD, Jain RK. Taxane- 513
 induced apoptosis decompresses blood vessels and lowers interstitial 514
 fluid pressure in solid tumors: clinical implications. *Cancer Res* 515
 1999;**59**:3776-3782. 516
13. Vlahovic G, Ponce AM, Rabbani Z, Salahuddin FK, Zgonjanin L, 517
 Spasojevic I, et al. Treatment with imatinib improves drug delivery and 518
 efficacy in NSCLC xenografts. *Br J Cancer* 2007;**97**:735-740. 519
14. Tufto I, Rofstad EK. Interstitial fluid pressure, fraction of necrotic tumor 520
 tissue, and tumor cell density in human melanoma xenografts. *Acta* 521
Oncol 1998;**37**:291-297. 522
15. Song CW, Kim MS, Cho LC, Dusenbery K, Sperduto PW. Radiobi- 523
 ological basis of SBRT and SRS. *Int J Clin Oncol* 2014;**19**:570-578. 524
16. Park HJ, Griffin RJ, Hui S, Levitt SH, Song CW. Radiation-induced 525
 vascular damage in tumors: implications of vascular damage in ablative 526
 hypofractionated radiotherapy (SBRT and SRS). *Radiat Res* 527
 2012;**177**:311-327. 528

- 529 17. Lovey J, Lukits J, Remenar E, Koroncay K, Kasler M, Nemeth G, et al. 550
530 Antiangiogenic effects of radiotherapy but not initial microvessel density 551
531 predict survival in inoperable oropharyngeal squamous cell carcinoma. 552
532 *Strahlenther Onkol* 2006;**182**:149-156. 554
- 533 18. Harrington KJ, Rowlinson-Busza G, Uster PS, Vile RG, Peters AM, 555
534 Stewart JS. Single-fraction irradiation has no effect on uptake of 556
535 radiolabeled pegylated liposomes in a tumor xenograft model. *Int J* 557
536 *Radiat Oncol Biol Phys* 2001;**49**:1141-1148. 558
- 537 19. Henriksen JR, Petersen AL, Hansen AE, Frankaer CG, Harris P, Elema 559
538 DR, et al. Remote loading of (64)Cu(2+) into liposomes without the use 560
539 of ion transport enhancers. *ACS Appl Mater Interfaces* 2015;**7**:22796- 561
540 22806. 562
- 541 20. Reyes-Aldasoro CC, Griffiths MK, Savas D, Tozer GM. CAIMAN: an 563
542 online algorithm repository for cancer image analysis. *Comput Methods* 564
543 *Programs Biomed* 2011;**103**:97-103. 565
- Q6 21. Fliedner FP, Hansen AE, Jorgensen JT, Kjaer A. The use of Matrigel has 566
545 no influence on tumor development or PET imaging in FaDu human 567
546 head and neck cancer xenografts. *BMC Med Imaging* 2016;**16**:5. 568
- 547 22. Znati CA, Rosenstein M, McKee TD, Brown E, Turner D, Bloomer WD, 569
548 et al. Irradiation reduces interstitial fluid transport and increases the 570
549 collagen content in tumors. *Clin Cancer Res* 2003;**9**:5508-5513. 571
23. Koukourakis MI, Koukouraki S, Giatromanolaki A, Archimandritis SC, 550
551 Skarlatos J, Beroukas K, et al. Liposomal doxorubicin and convention- 552
553 ally fractionated radiotherapy in the treatment of locally advanced non- 554
555 small-cell lung cancer and head and neck cancer. *J Clin Oncol* 556
557 1999;**17**:3512-3521. 558
24. Stapleton S, Milosevic M, Tannock IF, Allen C, Jaffray DA. The intra- 559
560 tumoral relationship between microcirculation, interstitial fluid pressure 561
562 and liposome accumulation. *J Control Release* 2015;**211**:163-170. 563
25. Stapleton S, Allen C, Pintilie M, Jaffray DA. Tumor perfusion imaging 564
565 predicts the intra-tumoral accumulation of liposomes. *J Control Release* 566
567 2013;**172**:351-357. 568
26. Stapleton S, Jaffray D, Milosevic M. Radiation effects on the tumor 569
570 microenvironment: implications for nanomedicine delivery. *Adv Drug* 571
572 *Deliv Rev* 2017;**109**:119-30. 573
27. Hagtvet E, Roe K, Olsen DR. Liposomal doxorubicin improves 574
575 radiotherapy response in hypoxic prostate cancer xenografts. *Radiat* 576
577 *Oncol* 2011;**6**:135. 578
28. Harrington KJ, Rowlinson-Busza G, Syrigos KN, Vile RG, Uster PS, 579
580 Peters AM, et al. Pegylated liposome-encapsulated doxorubicin and 581
582 cisplatin enhance the effect of radiotherapy in a tumor xenograft model. 583
584 *Clin Cancer Res* 2000;**6**:4939-4949. 585
586
587
588
589
590
591
592
593
594
595
596
597
598
599
600